14th IMEKO TC10 Workshop Technical Diagnostics
New Perspectives in Measurements, Tools and Techniques
for system's reliability, maintainability and safety
Milan, Italy, June 27-28, 2016

Non-contact measurement of the temperature profile of PET preforms

Bortolino Saggin[1]*, Luigi Buzzi[1], Luca Cornolti[1], Hermes Giberti[1], Marco Tarabini[1], Diego Scaccabarozzi[1]

[1] *Politecnico di Milano, Dipartimento di Meccanica, Via Previati 1/C, 23900 Lecco (Italy)*
bortolino.saggin@polimi.it.

***Abstract* – This paper describes a method for the measurement of the internal and external temperature profiles of PET preforms used in the Injection Stretch Blow Moulding (ISBM) process. Temperature is the most critical parameter for the process quality, but no online measuring system has yet been implemented. The proposed system is based on two thermopiles for the identification of the internal temperature profile and a thermal camera for the measurement of the external temperature profile. The adopted sensors have been individually calibrated and the measurement uncertainty budget proved that the sensor's instrumental uncertainty is not the actual limiting factor for the system accuracy. The main accuracy limitations derive from the emissivity of the materials of PET preforms. The use of average emissivity values increases the measurement uncertainty to 1.4 °C, a value that is judged acceptable in this specific application.**

I. INTRODUCTION

In recent years, the need of lowering the costs and the environmental impact of plastic bottles production has brought to a continuous reduction of the quantity of material used for the production of each specimen. This process is not straightforward, as the reduction of the bottles' thickness increases the risk of production wastes.
The most employed technology to produce polyethylene terephthalate (PET) bottles (1) is based on two stages. In the first one, a thick compact polymer preform is produced. In the second stage, called injection stretch blow moulding (ISBM), this preform follows a complex process. At first it is sent into an infrared (IR) oven where it is heated above the glass transition temperature of PET. The heated preform is then transfer into a mould, where it is stretched by a rod and blown with compressed air until it assumes the bottle shape. The dynamic of the stretch-blow phase is strongly affected by the visco-plastic properties of PET, which in turn strongly depend on the temperature (2). Consequently, there are oven parameters – such as the lamps intensities – that require tuning whenever the type of product changes and sometimes also during the routinely operation of an ISBM machine to compensate environmental conditions changes. This task would be effectively performed if a feedback control system could be implemented.
The first step for the complete automation the development of a system capable of measuring the preform temperature profile. This system should be applicable on the production line and should allow detecting the temperature of both the internal and external surfaces of the preform. This last requirement depends on the low thermal conductivity of PET (3) and by the heating process which allows for non-negligible thermal gradient across the preform thickness.
This work presents the design and validation of a measurement system matching the requirements for the ISBM machine temperature profile automatic control. The proposed system is based on infrared (IR) detectors, extensively used in many applications (4) (5) (6). The working temperature range in ISBM is between 75°C and 130°C, which are respectively the glass transition and crystallization temperatures limits (7). A breadboard of the proposed apparatus was tested on an industrial ISBM machine. The influence of the machine parameters was examined to assess the requirements about the system detection threshold and the adequacy of the designed system. The paper is organized as follows: the proposed measurement method is presented in section 2. Section 3 describes the experimental results, which are then discussed in section 4). The main findings of this work are eventually summarized in section 5.

II. MATERIAL AND METHODS

A. Materials

The non-contact temperature measurements were performed using an infrared camera, NEC TH7102WX (spectral range 8-14 μm) and the thermopiles General Electric ZTP-115 (spectral range 6-14 μm). The thermopiles were selected because of their small size in addition to their metrological characteristics, fully matching the requirements of our application. The thermal camera was the one available in our laboratory and has been extensively used in temperature measurement performed also on plastic materials (8), (9) but this class

of instrument (i.e. micro-bolometric detector 320x240 pixels) is nowadays the workhorse in IR mapping.
In the proposed setup, the IR camera is used to map the temperature of the external surface of the preform and two thermopiles are mounted on a support (Figure 1) which slides inside the preform. One of the thermopiles is scanning the lateral surface of the preform, while the other one is axially mounted and allows probing the preform bottom. The temperature is derived from the voltage measured by a four-wire circuit setup using a NI 9234 data acquisition board. Data are stored on a personal computer using a LabVIEW based software.

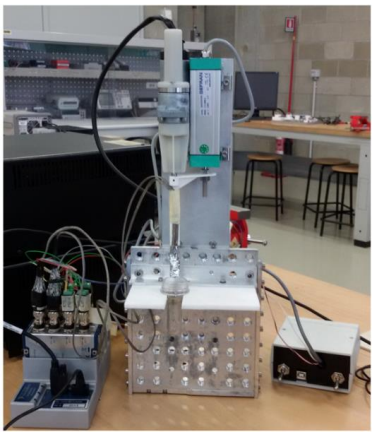

Figure 1. *Setup for the temperature profile scanning using thermopiles.*

This prototype measures the temperature of a preform taken out from the ISBM machine, but the system has been conceived to be eventually mounted directly on line. The PET preform selected as reference for the system validation is the one for the transparent 0.5 liter bottle. The global emissivity of PET is influenced by the degree of crystallinity (7), which depends on the production procedure and the geometry of the preform; consequently, it is important to characterize the preforms lot with respect to its emissivity. As preliminary investigation the emissivity of preforms of various shapes and colors were measured to investigate the possibility of using a single value of emissivity for all of them.

B. Preform characterization

The IR camera was used to measure the preforms emissivity using a Platinum resistance thermometer to obtain the actual temperature.
The output of the infrared camera is a corrected temperature (T_{out}), which corresponds to that of a black body having the same radiosity of the source. Starting from Stephan-Boltzmann equation, the relationship between incoming radiance, w_{net}, indicated temperature, T_{out} and the temperature of the body T_o is:

$$w_{net} = \sigma T_{out}^4 = \sigma \varepsilon_o T_o^4 + \sigma(1-\varepsilon_o)T_b^4 \qquad (1)$$

Where ε_o, T_o are respectively the emissivity and temperature of the investigated object, T_b is the background temperature and σ is the Stephan-Boltzmann's constant. Despite the adopted instruments are working in the 8-14 μm band, the total radiation pyrometer equations can be used because in the temperature range from 20 to 100 °C because the fraction of power within this band is almost constant. Eq. 1 can be rearranged to compute the object emissivity when the object and background temperatures are known:

$$\varepsilon_o = \frac{T_{out}^4 - T_b^4}{T_o^4 - T_b^4} \qquad (2)$$

In our tests, the preforms were heated to about 70°C, T_o and T_b were measured with Pt100 RTDs mounted respectively on the preform and the panel behind the camera. The experimental setup is shown in Figure 2. Using the above equation, the emissivity was measured on four samples for each preform lot.

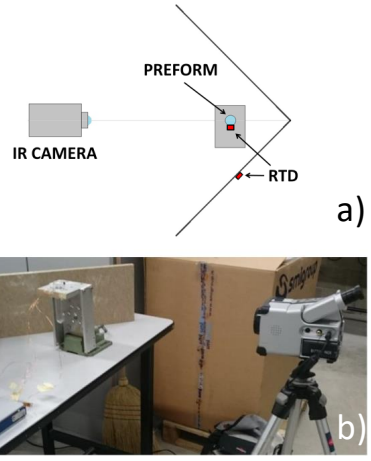

Figure 2. *Setup for the estimation of the emissivity of PET preform: a) scheme of the experimental system. b) Picture of the setup.*

III. SENSORS CALIBRATION.

In the thermopile, the detector is the common hot junction of a series of thermocouples, whose cold junction temperature is measured by an internal thermistor. In steady conditions the generated voltage across the junctions is directly proportional the incoming power, W_{net} that, in turn, is proportional to the difference of the forth power of the temperatures:

$$V = C(T_o^4 - T_s^4) \qquad (3)$$

Individual calibration (i.e. the identification of the constant C) is required for mass production detectors of the kind used in our application, because the manufacturer provides

only average values with uncertainty in the range of 10%. Since the measurement of the preform surface temperature requires a relative motion between the thermopile and the preform, it is important characterizing also the sensor dynamic behavior. The dynamic calibration was performed using the step input response: a shutter was interposed between a source at fixed temperature and the detector. As the thermopile behaves like a first order instrument (10), the response to the step input was used to determine the time constant.

A. Uncertainty budget

The instrumental uncertainty of the infrared camera was assessed in a previous work with a repeatability test (9). The repeatability was evaluated from the analysis of 300 frames of a black body. The determined standard deviation on each pixel of the frame, $u(T_{noise})$, can be approximated with a saddle function and reaches 0.2°C for the pixels near the edges of the array. The bias error in the range 0-100 °C was negligible in comparison to the repeatability. These figures allow reducing the instrumental uncertainty of about a factor 7 with respect to the manufacturer specification in the selected temperature range. The uncertainty of temperature measurements has to account also for the uncertainty of the object's emissivity and of the background temperature. All uncertainties have been evaluated using the A approach of the ISO GUM approach, for any measured parameter including emissivity and the thermopiles sensitivity.

For instance the uncertainty of the object temperature associated with the thermopiles $u(T_{o,p})$ is given by:

$$u(T_{o,p}) = \sqrt{\left(\frac{\partial T_0}{\partial \varepsilon_0}u(\varepsilon_0)\right)^2 + \left(\frac{\partial T_0}{\partial \Delta V}u(\Delta V)\right)^2 + \left(\frac{\partial T_0}{\partial C}u(C)\right)^2 + \left(\frac{\partial T_0}{\partial T_s}u(T_s)\right)^2}$$

$u(\varepsilon_0)$ is the uncertainty of the emissivity of the internal surface. The uncertainty of the calibration constant $u(C)$ is estimated through a least-square approach. To estimate the uncertainty of the output voltage $u(\Delta V)$, the standard deviation of measurements performed in repeatability condition was taken, being larger than the acquisition board specified instrumental uncertainty. Finally, the temperature of the sensor T_s was measured with the thermistor of the thermopile.

B. Breadboard performances validation

The measurement system described in the previous section was tested on an industrial ISBM machine manufactured by SMIgroup (11). The temperature profile of preforms leaving the infrared oven was measured for different machine configurations. The investigated parameters were selected among those that influence the heating process and can be controlled by the operator; these parameters were the intensity of the IR lamps and the production rate that determines the speed inside the oven.

Both parameters were initially set to the average values for standard production condition, and were afterwards modified by applying the minimal change that, according to the operators' experience, should induce a detectable effect on the bottles' quality. Table 1 shows the list of conditions characterizing the various tests. The intensity of individual layers of lamps was reduced by 5% with respect to the nominal value, referred to as "standard"; the decrease of the same amount was applied to the different layers of the IR oven (Figure 3). The line speed was reduced by 10% with respect to the standard condition to simulate a small change of the production rate. As can be seen in Table 1, the power of layer A was always kept at the standard value (i.e. maximum) as, according to the operator, the region near the ring was already close to the minimum in the test conditions.

***Table 1**. List of tests performed on the ISBM machine.*

Layer	Case 1	Case 2	Case 3	Case 4	Case 5	Case 6
A	Ref	Ref	Ref	Ref	Ref	Ref
B and C	Ref	-5%	Ref	Ref	-5%	Ref
D and E	Ref	Ref	-5%	Ref	Ref	-5%
Speed	Ref	Ref	Ref	-10%	-10%	-10%

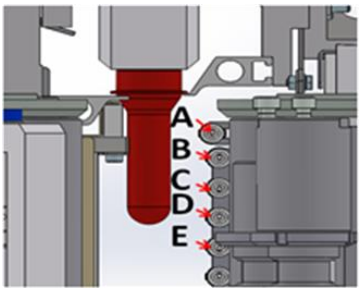

***Figure 3**. Scheme of the heating module of the ISBM machine.*

The temperatures measured by the thermal camera were statistically analyzed on the region shown in Figure 4; the area was 76 x 5 pixels in size. The maximum variation within the same row was 0.25°C. The temperature profile along the vertical line is similar to the one obtained by the thermopile.

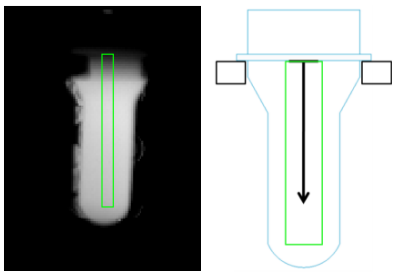

***Figure 4**. Example of image taken from the IR camera (left) and sketch of the region analyzed (right).*

IV. RESULTS

A. Preform characterization

The emissivity of the external surface of the reference preform samples are shown in Table 2, together with the standard uncertainty evaluated according to ISO GUM.

***Table 2**. Emissivity of the external and internal surfaces of the tested preforms and related measurement uncertainty*

Preform type	Emissivity	Uncertainty
1	0.872	0.008
2	0.861	0.008
3	0.870	0.008
4	0.889	0.008

The average emissivity is 0.873 with a standard deviation (reproducibility of experiments) of 0.012. This value is larger than the value that derives from the uncertainty analysis (0.008), so differences between the emissivity of preforms belonging to the same lot is inferred. For the inner surface, the parameter of interest is not actually the surface emissivity (that is likely to be the same of the outer surface) but a factor that includes the reflections of radiation from the surrounding part of the preform, generating the so called cavity effect of concave surfaces. The parameter was therefore determined from a radiative exchange model of the system.

B. Thermopiles characterization

The results of the static and dynamic calibration of the thermopiles are shown in Figure 5.

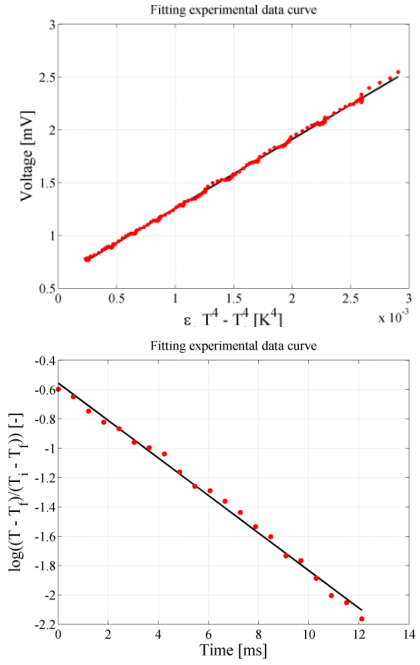

***Figure 5**. Calibration of the thermopile: upper plot: comparison of the least square fitting curve (Eq. 3) and the experimental data. Lower plot: estimation of the time constant (comparison between the linear fitting curve of Eq. 5 and the experimental data).*

The plots compare the theoretical results of Eq. 3 with the experimental data. The good agreement in both cases confirms that these models are representative of the actual thermopiles behavior. The calibration outlined a non-dimensional calibration constant $C = 0.654 \pm 0.015$, and time constant of 7.8 ± ms.

C. Uncertainty budget

Figure 6 shows the dependence of the object temperature uncertainty on the temperature itself, for both the IR camera (Eq. 6) and the thermopiles (Eq. 8).

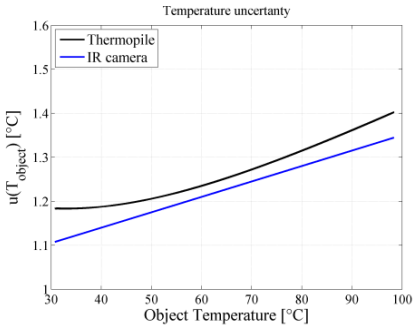

***Figure 6**. IR camera and thermopile estimated uncertainty as function of the investigated object temperature (Eq. 7 and Eq. 9).*

For both sensors, the main source of uncertainty is the emissivity, although the camera uncertainty (in the observed temperature range) is always lower than that of the thermopiles. At low temperatures, the voltage uncertainty of thermopiles is prevailing, but after 60°C, the trend becomes almost linear for both sensors. The constant relative uncertainty deriving from the emissivity is evident. The uncertainty increase with temperature is higher for the thermopiles, due to the contribution also of the calibration constant.

The breakdown of the uncertainty budget allows understanding whether it is necessary to identify the emissivity of each preform before the non-contact measurement or not. At 100°C the uncertainty using the average emissivity of the preform type is about 1.4°C; in the ideal case of the perfect knowledge of the preform emissivity ($u(\varepsilon_0) = 0$), this value would decrease to 0.5°C.

D. Preform temperature distribution

Figure 7 shows the measured temperatures of the external surface of the preform for conditions 1, 2, 3 and 4. The plot shows the temperature profiles (average of the three tests repetitions) in order to highlight the effects of the machine parameters. The data dispersion between the tests repetitions is highlighted by the dashed lines. One can

notice that the temperature repeatability does not allow distinguishing the effect of the change in the power of the layer D-E of the IR lamps. Conversely the change in the power of layers B-C is well evidenced

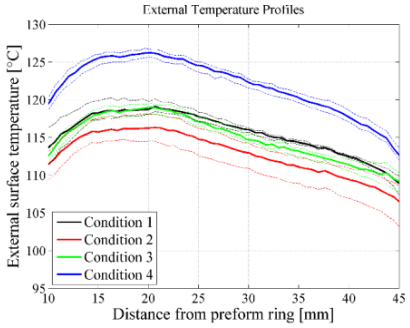

Figure 7*. Temperature profiles for conditions 1, 2, 3 and 4, dotted lines evidence the repeatability standard deviation.*

Figure 8 compares the means of internal and external temperature profiles.

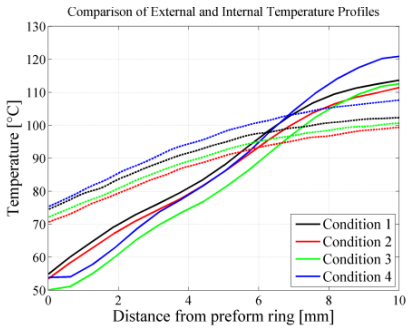

Figure 8*. Comparison of the averaged temperatures profile of the inner and outer surfaces for cases 1, 2, 3 and 4; solid lines represent the external profiles, dotted lines the internal.*

As the setup was designed to investigate the zone near the neck of the preform, which is the region where the differences between the external and internal temperatures are higher, only the 10 mm closest to the ring are reported.

V. DISCUSSION

The effectiveness of the proposed measurement system was evaluated by assessing the setup capability to detect the effect of minimal variations of machine settings. The discrimination threshold required to the system has been identified at first, then, the metrological performances of the measurement system have been compared with it.

A. ISBM Heating Process

The measurements results show that the temperature profiles are very similar to those considered ideal at the purpose of achieving a correct material distribution during the ISBM (12). The region close to the preform ring (neck region) is well below the glass transition temperature (75°C); then the temperature rapidly increases to values between 115°C and 120°C at a distance of 10 mm below the neck. Ideally, the PET below the ring should behave like a viscous material and should exhibit low resistance to deformation: the zone above the neck should not be deformed at all to keep the correct shape of the bottle cap. PET properties change along the preform length are obtained through a temperature gradient in this region. Starting from the hottest part, after a short plateau of about 10 mm, the temperature slowly decreases and in the last 30 mm the temperature is approximately 10°C lower than the maximum value.

In our tests, the parameter mostly affecting the temperature is the reduction of the production rate. The decrease of production rate by 10% (i.e. a longer staying within the IR oven) increased the temperature profile of about 9°C along all the preform. The reduction of the lamps intensities induces a minimal temperature reduction with respect to the standard condition. In particular, conditions 1 and 3 are very close, with a difference of about 1°C in the zone between 20 and 40 mm. In configuration 2, this deviation increases to 2-3°C, in agreement with the lamps arrangement. The results for conditions 5 and 6 (not reported in this work) are very close to condition 4, confirming the predominant effect of the production rate.

The differences of temperatures of the internal surface measured with different machine configuration are coherent with those observed on the external surface. The effect of the decreased production rate was smaller than that noticed on the external surface, given that the maximum temperature difference decreased from 10 °C of condition 1 to 6°C in condition 4. The comparison of temperatures on the internal and external surfaces of the preform shows that the inner temperature is always higher than the outer one in the region close to the ring of the preform, while after 6 mm the temperature gradient is reversed.

B. Measurement System

The uncertainty budget shows that the proposed system is not suitable to detect temperature differences smaller than 1.5°C. This implies that the machine settings 1 and 3 cannot be clearly discriminated, given that the temperature differences are comparable with the measurement uncertainty. The difference between settings 1 and 3 was a 5% reduction of the power of lamps D and E. The position of these lamps (Figure 3) is below the preform, that absorbs only a small fraction of the lamp radiation. The change of lamp power therefore entails a limited effect on the preform temperature. This effect is strictly related to the preform adopted, since longer preforms would be facing also the lamps of layers D and E. All the other

machine configurations led to temperature differences larger than the measurement uncertainty.

The main contribution to measurement uncertainty derives from uncertainty of the preform emissivity. Consequently, it is mandatory to characterize each lot of preforms in order to obtain more accurate temperature measurements.

Since the measured cooling rate is limited (less than 0.5 °C/s), the use of a moving thermopile is a good alternative to the IR camera to measure the temperature distribution also on the external surface. In our tests, performed with a non-optimized linear motor, the time duration of a measurement (descent – ascent) was less than 2 s; the cooling during the measurement was therefore comparable with the measurement uncertainty. In any case, the measurement time can be reduced by increasing the speed of the motor or by using an array of detectors; given their time constant, the adoption of fast motors would not lead to noticeable dynamic errors.

VI. CONCLUSIONS

In this work, we have described a method for the measurement of the internal and external temperature of preforms for ISBM. The method is based on infrared detectors and can be easily implemented on-board ISBM machines during the production phase. The system validation performed on an industrial ISBM machine indicates that the system allows detecting the changes of the temperature profile corresponding to the least significant change in the machine settings. The uncertainty budget proved that the proposed approach allows distinguishing temperature differences of a few degrees being the standard uncertainty 1.4°C; this value is satisfying, given that the finer machine tuning performed by the operator usually leads to temperature variations of 2 to 3 °C. Since the use of a wrong emissivity would lead to a systematic error, it would be anyway possible using the proposed system for temperature control once the optimal condition has been identified. The low cooling rate allowed for the use of a moving sensor with a scan time of about 1 s without significantly increasing the measurement uncertainty.

VII. ACKNOWLEDGEMENTS

The authors want to thank SMIgroup company for supporting this work and for providing the ISBM machine for our tests.

VIII. REFERENCES

[1] D.V. Rosato, A.V. Rosato, D.P. Di Mattia. Blow Molding Handbook: Technology, Performance, Markets, Economics. The Complete Blow Molding Operation. Cincinnati : Hanser Gardner, 2004.

[2] A.M. Adams, C.P. Buckley, D.P. Jones. Biaxial hot drawing of poly(ethylene terephthalate): measurements and modelling of strain-stiffening. Polymer. 2000, Vol. 41, pp. 771–786.

[3]S. Monteix, Y. Le Maoult, F. Schmidt, J.P. Arcens. Quantitative infrared thermography applied to blow moulding process: measurement of a heat transfer coefficient. Quantitative InfraRed Thermography Journal. 2004, Vol. 1, 2, pp. 133-150.

[4]A Stationary System of Noncontact Temperature Measurement and Hotbox Detecting. M.Z.Sreckovic, S.D. Milic and. 5, Sept 2008, Vehicular Technology, IEEE Transactions on, Vol. 57, pp. 2684-2694.

[5]Design of infrared temperature monitoring system applied to the stator of evaporative cooling hydrogenerators. Lin, Huang Jing and R. 2010. Electrical Machines and Systems (ICEMS), 2010 International Conference on. p. 1374-1377.

[6]Implementation of remote temperature-measuring by using a thermopile for Wireless Sensor Network. Huang, Chin-Fu Tsai and Wei-Sheng. 2012. Industrial Electronics and Applications (ICIEA), 2012 7th IEEE Conference on. p. 1325-1328.

[7]X.F. Lux, J.N. Hay. Isothermal crystallization kinetics and melting behaviour of poly(ethylene terephthalate). Polymer. 2001, Vol. 42, 23, pp. 9423-9431.

[8]Estimation of the orthosis-limb contact pressure through thermal imaging. M. Tarabini, B. Saggin, D. Scaccabarozzi and G. Lanfranchi. 2012. Instrumentation and Measurement Technology Conference (I2MTC), 2012 IEEE International. pp. 2733-2737.

[9]D. Scaccabarozzi, B. Saggin. About the dynamic characterization of micro-bolometric infrared cameras. Sensor and Actuator A. 2014, Vol. 217, pp. 68-74.

[10]H. Budzier, G. Gerlach. Thermal Infrared Sensor: Theory, Optimization and Practice. Chichester : John Wiley & Sons, 2011.

[11]http://www.smigroup.it. [Online]

[12]M. Bordival, F.M. Schmidt, Y. Le Maoult, V. Velay. Optimization of Preform Temperature Distribution for the Stretch-Blow Molding of PET Bottles: Infrared Heating and Blowing Modeling. Polymer Engineering & Science. 2009, Vol. 49, 4, pp. 783-793.